Available online at www.sciencedirect.com

ScienceDirect

IFAC Papers Online CONFERENCE PAPER ARCHIVE

IFAC PapersOnLine 51-27 (2018) 140–145

A Simplified Waveform Energetics Approach to Interpreting Arterial and Venous Pressure

Shaun M. Davidson*, Joel Balmer*, Chris Pretty*, Thomas Desaive, J. Geoffrey Chase***

**Department of Mechanical Engineering, University of Canterbury, Christchurch, New Zealand (e-mail: shaun.davidson@pg.canterbury.ac.nz)*

***GIGA-Cardiovascular Sciences, University of Liège, Liège, Belgium (e-mail: tdesaive@ulg.ac.be)*

Abstract: This paper develops a novel methodology for extracting simple, beat-to-beat, lumped metrics of systemic circulation performance by comparing the catheter pressure waveforms from the femoral artery and vena cava. Their diagnostic potential is compared to the similar, clinically used metric ΔMP, the drop in mean blood pressure between the aorta and vena cava, across an experimental cohort encompassing the progression of sepsis and several clinical interventions known to alter circulatory state. Both $O_{fe\rightarrow vc}$, the model derived pressure attenuation between the femoral artery and vena cava, and the clinical metric, ΔMP, performed well. However, $O_{fe\rightarrow vc}$ reduced the optimal average time to sepsis detection from endotoxin infusion from 46.2 minutes for ΔMP to 11.6 minutes, for a slight increase in false positive rate from 1.8% to 6.2%. Thus, the potential diagnostic benefits of this novel approach are demonstrated, and a case is made for further investigation.

Keywords: Bio-signal analysis, processing and interpretation; Cardiovascular system; Decision support systems

1. INTRODUCTION

Sepsis is a type of distributive shock that drives myocardial depression (Hunter and Doddi, 2010), and is a significant contributor to intensive care unit (ICU) admissions, with 10.4% of ICU admissions in the US attributed, and mortality, with an associated mortality rate of 20 – 50% (Martin et al., 2003). The effects of sepsis are often compounded by inadequate or incorrect diagnosis in the ICU, which leads to increased length of stay, cost and mortality, further inflating these figures (Angus et al., 2001; Pineda et al., 2001). ICU management of conditions, such as sepsis, frequently relies on information rich pressure measurements from catheters situated in the arteries and veins near the heart. However, despite the information rich nature of these waveforms, the use of catheters is not necessarily associated with improved clinical outcomes (Frazier and Skinner, 2008; Chatterjee, 2009).

One of the possible reasons for this outcome is the ability of the human mind to simultaneously track only three to four variables effectively (Halford et al., 2005). ICU clinicians are frequently presented with a far greater volume of information. Clinicians are thus forced to rely on simplifications of the large amount of measured information, such as mean pressures instead of pressure waveforms, to allow for easy and rapid interpretation of this information. Thus, improved methods for the simplification, abstraction and synthesis of clinical information from these waveforms to ensure the most relevant pieces of clinical information are extracted and presented to clinicians in an easy to interpret fashion has the potential to bring significant benefits to patient diagnosis and titration of treatment.

As a distributive shock condition, sepsis primarily effects the peripheral areas of the systemic circulation. Fortunately, pressure catheters are frequently situated in the systemic circulation in the ICU, popularly in the aorta, femoral artery or vena cava (Gershengorn et al., 2014b; Gershengorn et al., 2014a; Harvey et al., 2005). While the situation of catheters in the periphery itself is impossible due to the small diameter of peripheral blood vessels, the pressure wave passing from artery to vein via the periphery should be modulated by, and thus contain information on the condition of, these peripheral blood vessels. This paper explores a means of extracting information about the condition of the systemic circulation by comparing associated arterial and venous pressure waveforms without fully modelling the circulatory system, an approach that could offer significant insight for relatively little effort.

There are several popular, existing methods for the comparison of input and output waveforms, such as arterial and venous pressures. Among the most common are transfer functions, frequently generated using fast Fourier transforms (Welch, 1967) or empirical mode decomposition (Huang et al., 1998). While both approaches have proven effective at information extraction, neither is able to effectively incorporate the extensive *a-priori* knowledge available about the circulatory system, or directly account for the effects on either waveform by active circulatory components such as the heart. In addition, transfer functions output a full spectra for each heartbeat analysed, which is not necessarily easier to rapidly interpret in a clinical environment than the catheter waveform itself. An

10.1016/j.ifacol.2018.11.653

ideal method output would be more similar to the lumped waveform approximations currently favoured in clinical practice, such as mean arterial pressure (MAP) and mean venous pressure (MVP) (Hall, 2010).

Thus, this paper explores a novel method for providing simple, lumped values that are easy to rapidly interpret, but retain more of the underlying physiological information from the catheter pressure waveform. The method focuses on the relative changes in pulse wave amplitude and steady state values between analogous areas of the femoral artery and vena cava pressure waveforms. Comparison between method outputs and established clinical metrics is performed across an experimental data set including the progression of sepsis, a diverse, important and difficult to diagnose condition (Poeze et al., 2004; Dellinger et al., 2013).

2. METHODS

There are significant differences between the Femoral Pressure (P_{fe}) and Central Venous Pressure (P_{vc}) waveforms, both in terms of magnitude and shape. As previously discussed, the capillary beds of the peripheral systemic circulation lie between the femoral artery and vena cava, and the small vessel diameter results in a significant decrease in blood flow and pressure (Hall, 2010). Thus, the pressure pulse in P_{fe} is converted into flow in the capillaries, and then back into a reduced magnitude pulse in P_{vc}. This reduced magnitude pressure pulse in P_{vc} is also heavily influenced by downstream right heart behaviour, an influence which must be mitigated when interpreting P_{vc} as a result of upstream P_{fe}. This task can be accomplished by specifically using the region between the 'V' peak and 'Y' trough of P_{vc}, as shown in Fig. 1, for a linear least squares comparison with the analogous region of P_{fe}. The 'A' and 'C' peaks, also shown in Fig. 1, are the result of downstream right heart behaviour (Hall, 2010), and thus ignored.

While the pressure pulse is not transferred directly through the periphery from P_{fe} to P_{vc}, mean pressure is in an attenuated form. However, due to the reduced blood flow in the periphery, the i^{th} beat of P_{fe} ($P_{fe,i}$) and i^{th} beat of P_{vc} ($P_{vc,i}$) do not correspond to one another. Thus, $P_{fe,i}$ must instead be compared to a $P_{vc,i+j}$, where j represents the number of heartbeats' time the pressure wave takes to pass through the systemic circulation. The value of j can be determined on a subject specific basis by solving the optimisation problem:

$$j = \text{argmin}_j \left\| \left[\max\left(\dot{P}_{vc,i+j}\right)\right] - \left[\max\left(\dot{P}_{fe,i}\right)\right] \right\|_2 \qquad (1)$$

This optimisation problem seeks to find j, such that directional peak-to-peak variation in P_{fe} and P_{vc} is in best agreement. The logic behind Eq. 1 being, if one is interpreting P_{vc} as an output from P_{fe}, then it stands to reason that relative, inter-beat fluctuations due to other, lower frequency influences, such as breathing, should be preserved between the two waveforms. While j is unconstrained when solving in Eq. 1, it is consistently found to be $j = 3$ or 4 across the experimental data set assessed, supporting the physiological validity of this approach. This value for j should remain constant for a given, continuously monitored subject, as each pressure pulse passed into the periphery must, in turn, exit it.

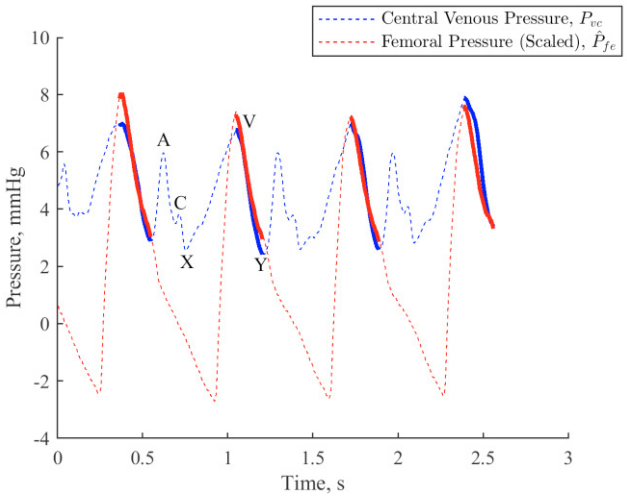

Fig. 1. Linear least squares alignment of scaled P_{fe} and P_{vc}. Regions used for the linear least squares fit are bolded. The P_{vc} peaks 'A', 'C' and 'V', and troughs 'X' and 'Y' are labelled for a single beat.

2.1 The Novel Method: Comparing P_{fe} with P_{vc}

For every fourth heartbeat, i, the comparison between P_{fe} and P_{vc} is performed via:

1. Take the set of four heartbeats of femoral pressure $P_{fe,i}$ to $P_{fe,i+3}$, and the associated set of four heartbeats of vena cava pressure $P_{vc,i+j}$ to $P_{vc,i+j+3}$. j represents the subject specific number of heartbeats' time a pressure wave takes to pass through the systemic circulation, as determined in Eq. 1.

2. Determine the phase lag, additional to the number of heartbeats' phase lag expressed by j, by comparing the peak and trough timing of P_{fe} and P_{vc}:

$$\delta_{fe\rightarrow vc} = \text{mean}\left(\begin{bmatrix} t_{\max(P_{vc},i+j)} - t_{\max(P_{fe},i)} \\ \vdots \\ t_{\max(P_{vc},i+j+3)} - t_{\max(P_{fe},i+3)} \\ t_{\min(P_{vc},i+j)} - t_{\min(P_{fe},i)} \\ \vdots \\ t_{\min(P_{vc},i+j+3)} - t_{\min(P_{fe},i+3)} \end{bmatrix} \right) \qquad (2)$$

   where $t_{\max(Pvc)}$ is the timing of the P_{vc} 'V' peak, and $t_{\min(Pvc)}$ the timing of the P_{vc} 'Y' trough. $\delta_{fe\rightarrow vc}$ represents the amount of time, additional to j heartbeats, by which P_{vc} lags P_{fe}.

3. Align the peaks and troughs of P_{fe} and P_{vc} by shifting P_{fe} to the right by j heartbeats, in addition to $\delta_{fe\rightarrow vc}$. This modified P_{fe} is referred to henceforth as $\hat{P}_{fe}$.

4. Perform linear least squares on the analogous regions of of $\hat{P}_{fe}$ and P_{vc}, highlighted in Fig. 1, to find:

$$\begin{bmatrix} \begin{pmatrix} \hat{P}_{fe}\left(t_{max(P_{vc},i+j)}\right) \\ \vdots \\ \hat{P}_{fe}\left(t_{min(P_{vc},i+j)}\right) \end{pmatrix} & 1 \\ \vdots & \vdots \\ \begin{pmatrix} \hat{P}_{fe}\left(t_{max(P_{vc},i+j+3)}\right) \\ \vdots \\ \hat{P}_{fe}\left(t_{min(P_{vc},i+j+3)}\right) \end{pmatrix} & 1 \end{bmatrix} \times \begin{bmatrix} A_{fe\to vc} \\ \Delta_{fe\to vc} \end{bmatrix} = \begin{bmatrix} \begin{pmatrix} P_{vc}\left(t_{max(P_{vc},i+j)}\right) \\ \vdots \\ P_{vc}\left(t_{min(P_{vc},i+j)}\right) \end{pmatrix} \\ \vdots \\ \begin{pmatrix} P_{vc}\left(t_{max(P_{vc},i+j+3)}\right) \\ \vdots \\ P_{vc}\left(t_{min(P_{vc},i+j+3)}\right) \end{pmatrix} \end{bmatrix} \quad (3)$$

$A_{fe\to vc}$ represents the relative pressure-pulse amplitude of P_{fe} and P_{vc}, and $\Delta_{fe\to vc}$ the associated identification offset.

These terms allow P_{vc} to be constructed as a scaled P_{fe} waveform, independent of downstream right heart influences, as shown in Fig. 1.

5. As $A_{fe\to vc}$ scales the entire P_{fe} waveform, thus trading off with $\Delta_{fe\to vc}$, $\Delta_{fe\to vc}$ does not provide an independent estimate of the pressure drop between the two waveforms. Instead, $O_{fe\to vc}$, the pressure drop between the original P_{fe} waveform and the P_{vc} waveform reconstructed using P_{fe}, which is independent of downstream influence from the right heart, is calculated using:

$$O_{fe\to vc} = \text{mean}\left(\begin{bmatrix} \hat{P}_{fe}\left(t_{\text{start}(\hat{P}_{fe},i)}\right) & 1 \\ \vdots & \vdots \\ \hat{P}_{fe}\left(t_{\text{end}(\hat{P}_{fe},i+3)}\right) & 1 \end{bmatrix} \times \begin{bmatrix} A_{fe\to vc} \\ \Delta_{fe\to vc} \end{bmatrix} - \begin{bmatrix} \hat{P}_{fe}\left(t_{\text{start}(\hat{P}_{fe},i)}\right) \\ \vdots \\ \hat{P}_{fe}\left(t_{\text{end}(\hat{P}_{fe},i+3)}\right) \end{bmatrix}\right) \quad (4)$$

The simplified, waveform derived parameters of interest are the relative amplitude, $A_{fe\to vc}$, and direct pressure offset, $O_{fe\to vc}$.

2.2 Experimental Data

The experimental protocol presented here was approved by the Institutional Animal Care and Use Ethics Committee of the University of Liège, Belgium (Reference Number 14-1726). A cohort of five male, Piétrain pigs were sedated, anesthetised and mechanically ventilated (GE Engstrom CareStation). Measurement of aortic (P_{ao}), femoral (P_{fe}) and central venous (P_{vc}) pressures was performed via pressure catheter (Transonic, NY, USA) at a sampling rate of 250 Hz. The experimental protocol included:

- Endotoxin infusion model of sepsis (lipopolysaccharide from E. Coli, 0.5 mg/kg, infused over 30 mins). Sepsis leads to an inflammatory response and capillary leakage, in turn resulting in hypovolemia, tissue hypoxia, and cardiac failure (Nguyen et al., 2006). As such, sepsis would be expected to cause significant changes in the systemic circulation, and thus the P_{fe} and P_{vc} waveforms.
- A number of lung recruitment manoeuvres, performed both before and after the endotoxin infusion. Recruitment manoeuvres drive changes in preload, and are often associated with decreased mean blood pressure and cardiac output (Jardin et al., 1981).
- Several fluid infusions (500 mL saline over 30 minutes), performed both before and after the endotoxin infusion. These fluid infusions served as simulations of fluid resuscitation therapy, a key hemodynamic resuscitation technique, associated with an increase in circulatory volume (Boyd et al., 2011; Vincent and Gerlach, 2004; Schierhout and Roberts, 1998; Stewart et al., 2009; Kastrup et al., 2007).

Once sepsis driven circulatory failure was sufficiently advanced, data was discarded due to the significant degradation of arterial and venous pressure waveforms. Due to varied responses to the endotoxin infusion, this cut off point varied, and not all pigs completed the entire clinical protocol. Every data set contains at least 5,000 heartbeats.

2.3 Analyses

The clinical metric most closely analogous to the metrics derived from the method presented in this paper is ΔMP = MAP – MVP, in this paper calculated using mean P_{ao} for MAP and mean P_{vc} for MVP. ΔMP is a surrogate for systemic resistance (Hall, 2010), similar to the derived $O_{fe\to vc}$ presented. The diagnostic sensitivity and specificity of the clinical and novel metrics was assessed using Receiver Operator Characteristic (ROC) curves (Wright, 2005). The following process, illustrated in Fig. 2, was used to generate these ROC curves:

1. Generate a baseline median value for each metric using the first 30 minutes of data recorded.
2. Divide the remaining data into 10 minute samples with rolling, 1 minute start points. Take the median value of each metric for each sample. Omit the 10 minutes of data directly following endotoxin infusion, as this data cannot easily be classified as ‘healthy’ or ‘sepsis’.
3. Classify all samples prior to the beginning of endotoxin infusion as ‘healthy’, and all samples after 10 minutes post endotoxin infusion as ‘sepsis’.
4. Generate the ROC curve using a range of thresholds relative to the subject and metric specific baseline median value.

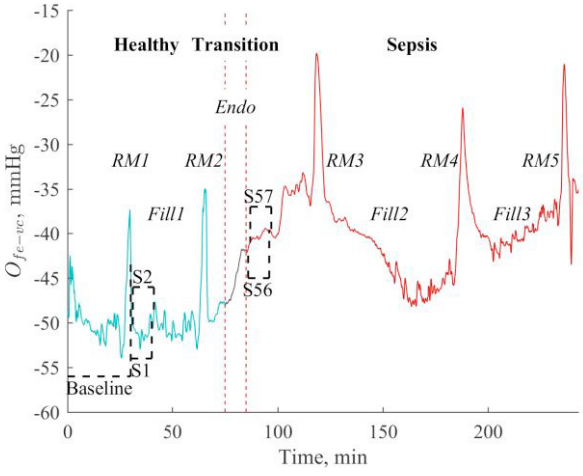

Fig. 2. The various sample regions used to develop the ROC curves. ‘Baseline’ represents the 30 minute baseline, S1, S2,… 10 minute ‘healthy’ samples, and S56, S57,… 10 minute ‘sepsis’ samples. ‘Endo’ represents an endotoxin infusion, ‘RM’ a recruitment manoeuvre, and ‘Fill’ a fluid infusion.

The comparison between the method derived metrics and clinical metrics using these ROC curves involved three major components:

1. Direct evaluation of the ROC curve results, and especially the proximity to the ideal sensitivity and specificity of 1.0 achievable across the full range of diagnostic thresholds trialled for each metric.

2. Evaluation of aggregate ROC performance for each metric, the traditional approach to which involves the summation of areas under the curve, providing an indication of potential metric performance across all diagnostic thresholds. However, in this study the focus is on evaluating the potential diagnostic capability of each metric when the same *a-priori* threshold is employed across all subjects, as this is likely how the method would be clinically implemented. This is achieved by evaluating the proximity for a given metric to a sensitivity and specificity of 1.0 across all diagnostic thresholds, k, which, for a given pig, i, can be expressed:

$$\varepsilon_i(k) = \left\| \begin{bmatrix} (1 - sensitivity(k)) \\ (1 - specificity(k)) \end{bmatrix} \right\|_2 \quad (5)$$

   Taking the mean of ε_i across all pigs, i, provides a measure of the overall proximity to a sensitivity and specificity of 1.0 achievable for a given metric using an *a-priori* threshold, as would be the case clinically.

3. An evaluation of the rapidity with which each metric could detect sepsis after endotoxin infusion occurred, when using the optimum *a-priori* threshold determined in the previous evaluation. As sepsis is a fast acting condition, rapid diagnosis can have a significant effect on patient outcomes (Dellinger et al., 2013). Hence, a shorter time to detection, all else equal, is desirable.

3. RESULTS

The ROC plots comparing the clinical and novel metrics for each pig are presented in Fig. 3. Metric performance appears to vary notably between pigs, and each metric achieves a sensitivity and specificity of 1.0 for at least one pig. Some ROC curves appear to end prematurely due to the use of the baseline median reading, as opposed to a reading of zero, as a diagnostic comparator. In general, both $O_{fe\rightarrow vc}$ and ΔMP demonstrate strong, consistent performance, with $A_{fe\rightarrow vc}$ performing relatively poorly. However, a quantitative comparison of the overall performance of these metrics is difficult to establish from the ROC plots themselves.

Fig. 4 provides such a quantitative comparison. This figure shows the proximity to a sensitivity and specificity of 1.0 achievable when the same *a-priori* threshold, across a range of 1% - 400% of the subject-specific baseline median reading for a given metric, is used across all pigs. Fig. 4 clearly demonstrates the strong performance of $O_{fe\rightarrow vc}$ and ΔMP, and relatively poor, inconsistent performance of $A_{fe\rightarrow vc}$.

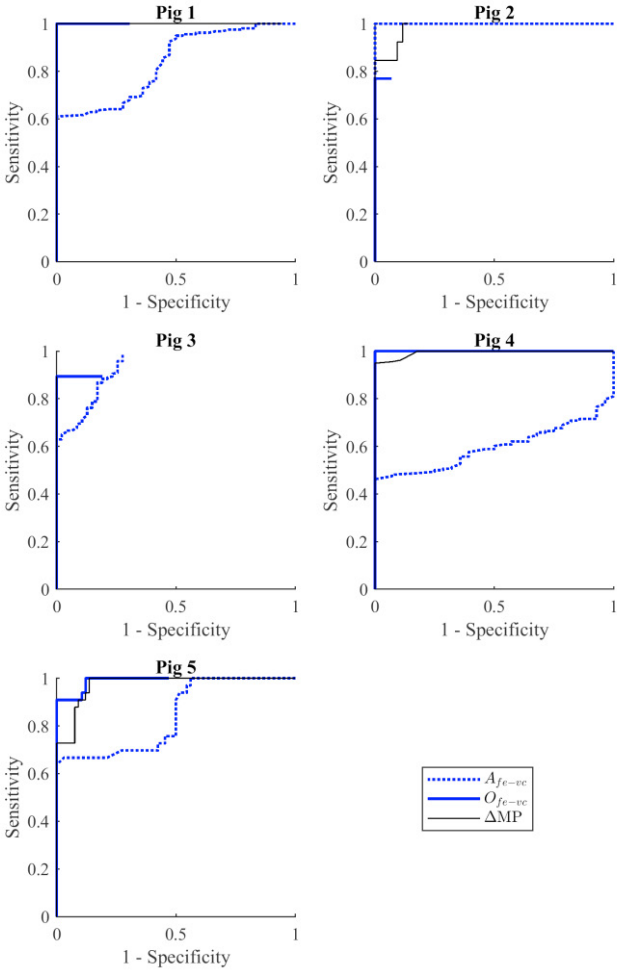

Fig. 3. ROC curves across all 5 pigs for the clinical metric ΔMP, and novel metrics $A_{fe\rightarrow vc}$ and $O_{fe\rightarrow vc}$.

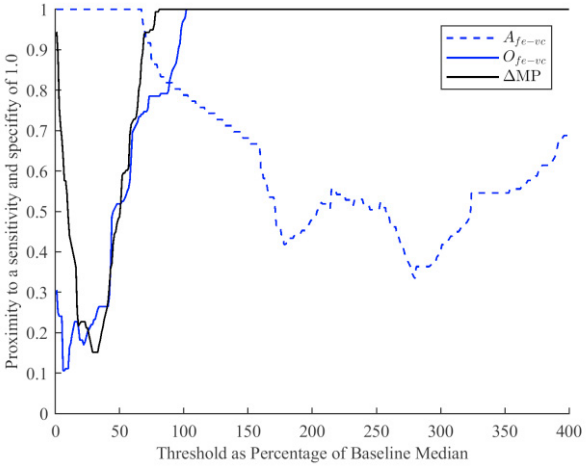

Fig. 4. Proximity to a sensitivity and specificity of 1.0 (lower is better) when an *a-priori* threshold, relative to the baseline median sample, is used across all pigs.

Finally, Table 1 shows the rapidity with which each metric was able to detect sepsis after the endotoxin infusion using the optimal *a-priori* threshold from Fig. 4, along with the

percentage of false positives reported prior to endotoxin infusion using this threshold. There is a clear trade-off in Table 1 between rapid diagnosis, but lower specificity, and slower diagnosis, but a greater degree of specificity.

Table 1. Time (*t*), in minutes, to sepsis detection after endotoxin infusion using the thresholds established in Fig. 4, and the percentage of false positives (%FP) reported prior to endotoxin infusion.

Pig	$A_{fe\rightarrow vc}$		$O_{fe\rightarrow vc}$		ΔMP	
	t	%FP	*t*	%FP	*t*	%FP
Pig 1	168	0.0	8	0.0	33	0.0
Pig 2	14	0.0	17	0.0	22	0.0
Pig 3	131	0.0	31	0.0	68	0.0
Pig 4	148	0.0	1	3.6	94	0.0
Pig 5	29	0.0	1	27.3	14	9.1
Mean	98.0	0.0	11.6	6.2	46.2	1.8

4. DISCUSSION

The ROC curves in Fig. 3 demonstrate the potential performance of each metric on each pig across the full range of diagnostic thresholds assessed. These curves demonstrate both the variability of metric performance across pigs, and the relatively strong performance of metrics ΔMP and $O_{fe\rightarrow vc}$, as well as the more variable performance of metric $A_{fe\rightarrow vc}$. While a direct quantitative comparison of the three metrics using the ROC curves themselves is difficult, these curves form the foundation for subsequent comparisons.

The first of these aggregate, quantitative comparisons is presented in Fig. 4. Here, the proximity to a specificity and sensitivity of 1.0 for each metric when the same *a-priori* threshold, relative to the baseline median reading, is used across all pigs. The novel metric $O_{fe\rightarrow vc}$ delivers the overall best performance at a diagnostic threshold of a 6 – 11% positive shift from baseline median, closely followed by the clinical metric ΔMP at a diagnostic threshold of 29 – 33% positive shift from baseline median. $A_{fe\rightarrow vc}$, despite performing well on Pig 2 in Fig. 3, fails to present any *a-priori* diagnostic threshold that is consistently effective across the experimental cohort.

Both the breadth and location of the optimal diagnostic threshold regions in Fig. 4 is important. The breadth indicates some level of metric resilience to sub-optimal diagnostic threshold selection, and the location roughly a trade-off between specificity, at higher thresholds, and sensitivity, at lower thresholds. The breath of the optimal diagnostic regions of $O_{fe\rightarrow vc}$ and ΔMP are similar (6 – 11% and 29 – 33%, respectively), but their location quite different. While Fig. 4 does not directly separate between specificity and sensitivity, and thus does not allow comparison of the trade-offs between these different optimal regions, Table 1 does.

Table 1 presents the rapidity with which each metric is able to detect sepsis after endotoxin infusion, an indication of sensitivity, and the percentage of false positives reported prior to endotoxin infusion, an indication of specificity. While the results presented in Table 1 are not identical to actual sensitivity or specificity, they have been selected for their clinical relevance (for example, false negatives after a sepsis diagnosis are likely of less clinical importance). Here, the aforementioned trade-off between sensitivity and specificity in $O_{fe\rightarrow vc}$, with a mean detection time of 11.6 minutes, but a mean false positive rate of 6.2%, and ΔMP, with a mean detection time of 46.2 minutes and a mean false positive rate of 1.8%, is demonstrated.

While neither $O_{fe\rightarrow vc}$ nor ΔMP are universally superior, a strong case can be made for the advantages of the metric $O_{fe\rightarrow vc}$. Fig. 4 shows that, at its optimum threshold and with sensitivity and specificity given equal weighting, $O_{fe\rightarrow vc}$ provides overall superior performance to ΔMP at its respective optimum threshold. Table 1 shows $O_{fe\rightarrow vc}$ has advantages in sensitivity, and ΔMP in specificity. Sepsis acts rapidly (Hall, 2010). Thus, the shift in average time to diagnosis from 11.6 minutes to 46.2 minutes could have significant impact on patient outcomes (Dellinger et al., 2013).

Conversely, the false positive rates for both metrics are low at 6.2% and 1.8%, sufficiently low that neither is likely to have similar clinical significance to the disparity in average sepsis detection times. This reduced time to detection for $O_{fe\rightarrow vc}$ when compared to ΔMP, due to the lower diagnostic threshold of $O_{fe\rightarrow vc}$, would suggest the novel method succeeds in reducing the influence of right heart behaviour on the P_{vc} waveform, thus allowing a clearer picture of underlying systemic circulation behaviour. Reducing the diagnostic threshold of ΔMP until the false positive rate exceeds that of $O_{fe\rightarrow vc}$ yields a diagnostic threshold of 13%, and a false positive rate of 6.4%. At this threshold, the average time to detection for ΔMP is 16.0 minutes, significantly lower than at the 29% threshold optimum point, but still 38% higher than the average detection time for $O_{fe\rightarrow vc}$. Further, this shift away from the optimum detection point for ΔMP results in a significant increase in false negatives after sepsis detection.

There are several study limitations to be noted. First, one of the major difficulties in clinical diagnosis of sepsis is in distinguishing sepsis from other, similar conditions (Poeze et al., 2004). While the data employed in this study is high quality, and included a variety of clinical interventions altering circulatory state, no other disease states were incorporated into the clinical protocol. This lack of other disease states is an important consideration, and the specificity and sensitivity results presented in this paper represent an initial study of the ability of this method to detect sepsis, rather than distinguish between various disease states. It is worth noting current sepsis diagnosis guidelines incorporate a variety of different metrics (Dellinger et al., 2013; Nguyen et al., 2006), including arterial pressure. Thus, the metrics presented in this paper, as demonstrated, may be better posed to replace these arterial pressure metrics as part of a larger diagnostic framework, rather than serve as independent diagnostic tools. A further limitation is that the study only includes data collected from pigs, rather than humans. As always, this limitation does allow the ability to explore induced, controlled and fully instrumented disease states, providing an excellent, rigorous data set for an initial feasibility study.

Overall, the novel metric $O_{fe \rightarrow vc}$, corresponding to the model derived pressure drop between the femoral artery and vena cava, provided compelling results relative to the clinically established metric of ΔMP for the diagnosis of sepsis. This novel metric relies on instrumentation typically available in a clinical environment. It thus has the potential to provide diagnostic benefits in a clinical environment at little additional cost.

5. CONCLUSIONS

This paper develops simple, easily interpretable metrics of systemic circulation performance by comparing the pressure waveforms from the femoral artery and vena cava. Performance of these metrics was compared to the analogous clinical metric ΔMP across an experimental data set incorporating the progression of sepsis, as well as several clinically standard interventions. The novel metric $O_{fe \rightarrow vc}$, the model derived pressure drop between the femoral artery and vena cava, provided a reduction in average time to sepsis detection, relative to ΔMP, from 46.2 minutes to 11.6 minutes, for a modest increase in false positive rate from 1.8% to 6.2%. Overall, this novel metric demonstrated stronger performance than the clinical metric ΔMP across the experimental cohort, providing a case for the further evaluation of its clinical usefulness and potential diagnostic benefits.

REFERENCES

Angus DC, Linde-Zwirble WT, Lidicker J, et al. (2001) Epidemiology of severe sepsis in the United States: analysis of incidence, outcome, and associated costs of care. *Critical Care Medicine* 29: 1303-1310.

Boyd JH, Forbes J, Nakada T-a, et al. (2011) Fluid resuscitation in septic shock: a positive fluid balance and elevated central venous pressure are associated with increased mortality. *Critical Care Medicine* 39: 259-265.

Chatterjee K. (2009) The swan-ganz catheters: past, present, and future a viewpoint. *Circulation* 119: 147-152.

Dellinger RP, Levy MM, Rhodes A, et al. (2013) Surviving Sepsis Campaign: international guidelines for management of severe sepsis and septic shock, 2012. *Intensive Care Medicine* 39: 165-228.

Frazier SK and Skinner GJ. (2008) Pulmonary artery catheters: state of the controversy. *Journal of Cardiovascular Nursing* 23: 113-121.

Gershengorn HB, Garland A, Kramer A, et al. (2014a) Variation of arterial and central venous catheter use in United States intensive care units. *The Journal of the American Society of Anesthesiologists* 120: 650-664.

Gershengorn HB, Wunsch H, Scales DC, et al. (2014b) Association between arterial catheter use and hospital mortality in intensive care units. *JAMA Internal Medicine* 174: 1746-1754.

Halford GS, Baker R, McCredden JE, et al. (2005) How many variables can humans process? *Psychological Science* 16: 70-76.

Hall JE. (2010) *Guyton and Hall textbook of medical physiology*: Elsevier Health Sciences.

Harvey S, Harrison DA, Singer M, et al. (2005) Assessment of the clinical effectiveness of pulmonary artery catheters in management of patients in intensive care (PAC-Man): a randomised controlled trial. *Lancet* 366: 472-477.

Huang NE, Shen Z, Long SR, et al. (1998) The empirical mode decomposition and the Hilbert spectrum for nonlinear and non-stationary time series analysis. *Proceedings of the Royal Society of London A: mathematical, physical and engineering sciences*. The Royal Society, 903-995.

Hunter J and Doddi M. (2010) Sepsis and the Heart. *British Journal of Anaesthesia* 104: 3-11.

Jardin F, Farcot J-C, Boisante L, et al. (1981) Influence of positive end-expiratory pressure on left ventricular performance. *New England Journal of Medicine* 304: 387-392.

Kastrup M, Markewitz A, Spies C, et al. (2007) Current practice of hemodynamic monitoring and vasopressor and inotropic therapy in post-operative cardiac surgery patients in Germany: results from a postal survey. *Acta Anaesthesiologica Scandinavica* 51: 347-358.

Martin GS, Mannino DM, Eaton S, et al. (2003) The epidemiology of sepsis in the United States from 1979 through 2000. *New England Journal of Medicine* 348: 1546-1554.

Nguyen HB, Rivers EP, Abrahamian FM, et al. (2006) Severe sepsis and septic shock: review of the literature and emergency department management guidelines. *Annals of Emergency Medicine* 48: 54. e51.

Pineda LA, Hathwar VS and Grant BJ. (2001) Clinical suspicion of fatal pulmonary embolism. *CHEST Journal* 120: 791-795.

Poeze M, Ramsay G, Gerlach H, et al. (2004) An international sepsis survey: a study of doctors' knowledge and perception about sepsis. *Critical Care* 8: R409.

Schierhout G and Roberts I. (1998) Fluid resuscitation with colloid or crystalloid solutions in critically ill patients: a systematic review of randomised trials. *BMJ* 316: 961-964.

Stewart RM, Park PK, Hunt JP, et al. (2009) Less Is More: Improved Outcomes in Surgical Patients with Conservative Fluid Administration and Central Venous Catheter Monitoring. *Journal of the American College of Surgeons* 208: 725-735.

Vincent J-L and Gerlach H. (2004) Fluid resuscitation in severe sepsis and septic shock: an evidence-based review. *Critical Care Medicine* 32: S451-S454.

Welch P. (1967) The use of fast Fourier transform for the estimation of power spectra: a method based on time averaging over short, modified periodograms. *IEEE Transactions on audio and electroacoustics* 15: 70-73.

Wright DB. (2005) Receiver operating characteristics curves. *Encyclopedia of statistics in behavioral science*.